Tunnelling and Underground Space Technology 85 (2019) 294–306

Contents lists available at ScienceDirect

Tunnelling and Underground Space Technology

journal homepage: www.elsevier.com/locate/tust

An equivalent anchoring method for anisotropic rock masses in underground tunnelling

Min Gao[a], Zhengzhao Liang[a], Shanpo Jia[b,*], Yingchun Li[a,*], Xuexiang Yang[b]

[a] State Key Laboratory of Coastal and Offshore Engineering, Dalian University of Technology, Dalian 116024, China
[b] School of Urban Construction, Yangtze University, Jingzhou, Hubei 434023, China

ARTICLE INFO

Keywords:
Anisotropy
Layered rock mass
Equivalent anchoring method
Rock bolts
Multiple linear regression analysis

ABSTRACT

Rock bolting has been widely utilized for reinforcing underground openings, such as tunnels and mining. To ease the complexity of numerically simulating of the bolted rock mass, a novel method for equivalent anchoring simulates the reinforcement effect of the bolts by considering the anisotropic characteristics of the layered rock mass. The jointed material model in ABAQUS is improved by incorporating the anisotropy through the programming language FORTRAN. Based on the improved jointed material model, the equivalent anchoring parameters of the bolted layered rock masses are studied through a series of numerical tests. The numerical outcomes reveal that the improved jointed material model can be used to simulate the anisotropic features of the layered rock mass by comparing the classic and analytic solutions. The degree to which the supporting parameters affect the equivalent reinforcement performance are different in anisotropic rock masses, and the sensitivity of their influence is bolt length > bolt spacing > bolt diameter. Furthermore, an equivalent anchoring model for bolted rock masses (the formula of the improved parameter between the ratio of bolt length to tunnel diameter and the ratio of bolt diameter to bolt spacing) is proposed through numerical results analysis by the multiple linear regression method. An application case shows the field monitoring agreed well with the predicted vertical displacement of the tunnel demonstrating the feasibility of the proposed simulation method for the bolted rock mass. The results show the proposed method in this study can be conveniently utilized for efficient simulation of the mechanical behavior of bolted rock masses.

1. Introduction

Rock bolting has become a prevalent reinforcing approach for supporting surrounding rock masses in tunnelling, mining and other underground engineering projects for more than 100 years. The strength and stiffness of the rock masses can be increased substantially after rock bolts are installed. Ongoing bolting design depends heavily on empirical or semi-empirical approaches (Shen and Barton, 1997; Wong et al., 2004; Liu et al., 2016). Therefore, the mechanical behavior of the bolted rock masses still eludes quantitative representation. With rapid development of computing technology, the Finite Element Method (FEM) has been extensively employed to study the mechanism of the bolting (Bernaud et al., 2009; Li et al., 2016). Adequate modeling of the mechanical behavior of bolted rock masses with the FEM necessitates a functional constitutive model. However, an equivalent simulation method for bolted rock masses that will simplify the difficulty and computational complexity of the numerical simulation, needs to be further investigated.

Studies on the bolted rock mass emphasize the bonding capacity of the rock bolt, and the interface properties between the rock bolts and the rock mass through laboratory testing and analytical examination (Hyett et al.,1992; Kilic et al., 2002; Li et al., 2014; He et al., 2015; Ghadimi et al.,2015). Analytical models assessing the contribution of rock bolts to the shear strength of stratified or jointed rock masses were investigated in the past (Spang and Egger, 1990; Pellet and Egger, 1996; Cai and Zhao, 2004). The influence of bolt profile, diameter, length, and the mechanical properties of grouting materials on the pull-out load have also been examined (Karanam and Dasyapu, 2005; Kilic et al., 2003). However, most of studies focused on the mechanical properties of the interface between the bolt and rocks. Other investigations have emphasized the constitutive representation of the bolted rock mass. Some constitutive models for the layered rock masses supported with bolts have been proposed by treating the bolted rock mass as an equivalent continuum (Yang, 1994; Yang et al., 2001), Which accurately describe the mechanism of rock bolting and evaluate the reinforcement efficiency of rock bolts for the layered rock masses. And

* Corresponding authors.
E-mail addresses: jiashanporsm@163.com (S. Jia), yingchun_li@dlut.edu.cn (Y. Li).

https://doi.org/10.1016/j.tust.2018.12.017
Received 10 April 2017; Received in revised form 28 November 2018; Accepted 21 December 2018

many similar studies have been conducted on the constitutive relationships of the bolted rock mass from different viewpoints (Zhang and Liu, 2002; Ahmad and Soroush, 2005; Li et al., 2006, 2017; Maghous et al., 2012; Cai et al., 2015). Though the constitutive models of the bolted rock mass appear to be accurate, the implementation and subsequent computational process are quite time-consuming. Additionally, the simulation performance is not always reasonable due to the interaction of many bolt elements in the numerical model (Yang, 2004).

To simplify the numerical representation of the bolted rock mass, many investigations assume that the constitutive relationship of the bolted rock mass is not changed, but the mechanical parameters of the rock mass are strengthened when rock bolts are installed (Zhu and Ren, 2001; Indraratna and Kaiser, 1990; Zhu and Zheng, 1996; Osgouir, 2006; Meng et al., 2014). Zhu et al. (1988) found that the effect on the strength of the bolted rock mass was mainly due to the increase of the internal friction angle, but the cohesion remained nearly unchanged. Other researches have concluded that the cohesion and stiffness of the jointed rock mass were improved by rock bolts (Marence and Swoboda, 1995; Kim et al., 2006). These methods can be defined as the equivalent anchoring method. To date, there is still no consensus on which mechanical parameters of the bolted rock mass are improved. The improved mechanical parameters of the surrounding rock masses reinforced by rock bolts and the equivalent simulation methods were also investigated (Wu et al., 2012; Chen et al., 2014; Srivastava and Singh, 2015; Chen et al., 2015; Liu et al., 2017). The enhanced parameters of surrounding rock mass were used for FEM simulation in slope and tunnel engineering projects (Chen and Zhu, 2001; Cai et al., 2004; Bobet and Einstein, 2011). Revisiting the above literature indicated that the rock reinforcement effect could be equivalently simulated by improving the parameters of the surrounding rock masses, but the increased value of the parameters such as elastic modulus, cohesive and internal friction angles needs to be further investigated. No unified theory or formula can identify which parameters should be improved in simulating the anchoring process for tunnel engineering. Thus, the equivalent simulation method for the bolted rock masses should be further studied.

In many situations, the surrounding rock mass was assumed to be isotropic in the numerical modeling. However, the rock mass exhibits highly anisotropic features, especially for the layered rock masses. The existing experimental evidence indicated that the layered rocks, such as schist, shales and slates, displayed a strong anisotropy of strength and deformation, which was usually controlled by the orientation of bedding planes (Colak and Unlu, 2004; Donath, 1961; Horino and Ellickson, 1970; Mclamore and Gray, 1967; Ramamurthy, 1993). The anisotropic properties of layered rock mass were investigated by laboratory test, analytical methods and numerical simulations (Tien et al., 2000, 2001, 2006; Amadei and Pan, 1992; Amadei, 1996; Chen et al., 1998; Liang et al., 2005; Ghazvinian et al., 2013). Therefore, a reasonable constitutive relationship of the layered rock masses should also be needed before studying the equivalent anchoring method.

The primary objective of this paper is to propose an equivalent simulation method for the bolted rock mass in tunnel engineering. To achieve this objective, this paper is organized as follows: an anisotropic constitutive model of the layered rock mass is firstly developed. Then, the equivalent anchoring mechanism of the bolted rock masses is numerically studied with different cases, i.e., determining an improved mechanical parameter for the surrounding rock mass to simulate the effect of bolts. The equivalent simulation method for the bolted layered rock masses is proposed based on the numerical results through multiple linear regression analyses. The numerical analysis of an engineering case demonstrates the reasonableness of the equivalent simulation method for the bolted layered rock masses. Finally, the conclusions are presented.

2. Anisotropic constitutive model for the layered rock mass

2.1. Anisotropic parameters of the layered rock mass

The elastic modulus and Poisson's ratio of rocks depends highly on the inclination angle of the joints (The angle between the joints and horizontal line: θ) according to the experimental and analytical results from transversely isotropic and anisotropic rock materials (Zhao and Yao, 1990; Xi and Chen, 1994; Zhang, 2007; Huang et al., 2010; Liu et al., 2013). Amadei (1996) suggested that the stress matrix (σ_x, σ_y, σ_z, τ_{yz}, τ_{zx}, τ_{xy}), and strain matrix (ε_x,ε_y, ε_z, γ_{yz}, γ_{zx}, γ_{xy}) of the layered rock mass were not only related to the five elastic parameters (E_1,ν_1,E_2,ν_2,G_2) but also to the inclination angle of the joint set (θ):

$$\begin{bmatrix}\varepsilon_x\\ \varepsilon_y\\ \varepsilon_z\\ \gamma_{yz}\\ \gamma_{zx}\\ \gamma_{xy}\end{bmatrix}=\begin{bmatrix}a_{11} & a_{12} & a_{13} & a_{14} & a_{15} & a_{16}\\ a_{21} & a_{22} & a_{23} & a_{24} & a_{25} & a_{26}\\ a_{31} & a_{32} & a_{33} & a_{34} & a_{35} & a_{36}\\ a_{41} & a_{42} & a_{43} & a_{44} & a_{45} & a_{46}\\ a_{51} & a_{52} & a_{53} & a_{54} & a_{55} & a_{56}\\ a_{61} & a_{62} & a_{63} & a_{64} & a_{65} & a_{66}\end{bmatrix}\begin{bmatrix}\sigma_x\\ \sigma_y\\ \sigma_z\\ \tau_{yz}\\ \tau_{zx}\\ \tau_{xy}\end{bmatrix} \tag{1}$$

The relationship between axial stress (σ_y) and strain (ε_x,ε_y, ε_z) can be expressed as:

$$\varepsilon_x = a_{12}\sigma_y, \quad \varepsilon_y = a_{22}\sigma_y, \quad \varepsilon_z = a_{23}\sigma_y \tag{2}$$

where a_{12}, a_{22} and a_{23} are functions of the inclination angle θ and the five elastic parameters (E_1,ν_1,E_2,ν_2,G_2), through the following relationships:

$$a_{12} = \left(\frac{1}{E_1} + \frac{1}{E_2} + \frac{2\nu_2}{E_2} - \frac{1}{G_2}\right)\sin^2\theta\cos^2\theta - \frac{\nu_2}{E_2} \tag{3}$$

$$a_{22} = \frac{1}{E_1}\sin^4\theta + \frac{1}{E_2}\cos^4\theta + \left(\frac{1}{G_2} - \frac{2\nu_2}{E_2}\right)\sin^2\theta\cos^2\theta \tag{4}$$

$$a_{23} = -\frac{\nu_2}{E_2}\cos^2\theta - \frac{\nu_1}{E_1}\sin^2\theta \tag{5}$$

where E_1 and ν_1 are the elastic modulus and Poisson's ratio parallel to the transversely isotropic surfaces, respectively, and E_2,ν_2 and G_2 are the elastic modulus, Poisson's ratio, and shear modulus perpendicular to transversely isotropic surfaces, respectively. The five elastic parameters can be determined through uniaxial and triaxial experiments.

Then, the elastic parameters of each joint dip angle are given by:

$$E = \frac{1}{a_{22}}, \quad \nu_{yz} = -\frac{a_{23}}{a_{22}}, \quad \nu_{yx} = -\frac{a_{12}}{a_{22}} \tag{6}$$

Both the elastic modulus and Poisson's ratio vary as functions of the joint dip angles:

$$\begin{cases} E(\theta) = f_1(\theta) \\ \nu(\theta) = f_2(\theta) \end{cases} \tag{7}$$

2.2. The improved jointed material model

The jointed material model employed by ABAQUS allows for the opening and frictional sliding of the joints. Additionally, the model includes a bulk material failure mechanism based on the Drucker-Prager failure criterion (ABAQUS Inc., 2012). To consider the anisotropic nature of the jointed rock mass, the jointed material model in ABAQUS has been modified by introducing the anisotropic parameters of the layered rock mass (Eqs. (1)–(7)). The FORTRAN language is utilized for the model implementation, and ABAQUS served as the calculator for simulating the layered rock mass.

Fig. 1 shows the calculation process for implementing the modified model. The subroutine is comprised of four steps, including the determination of the five layered rock mass elastic parameters, calling the calculations results of stress matrix at each increment, calling the

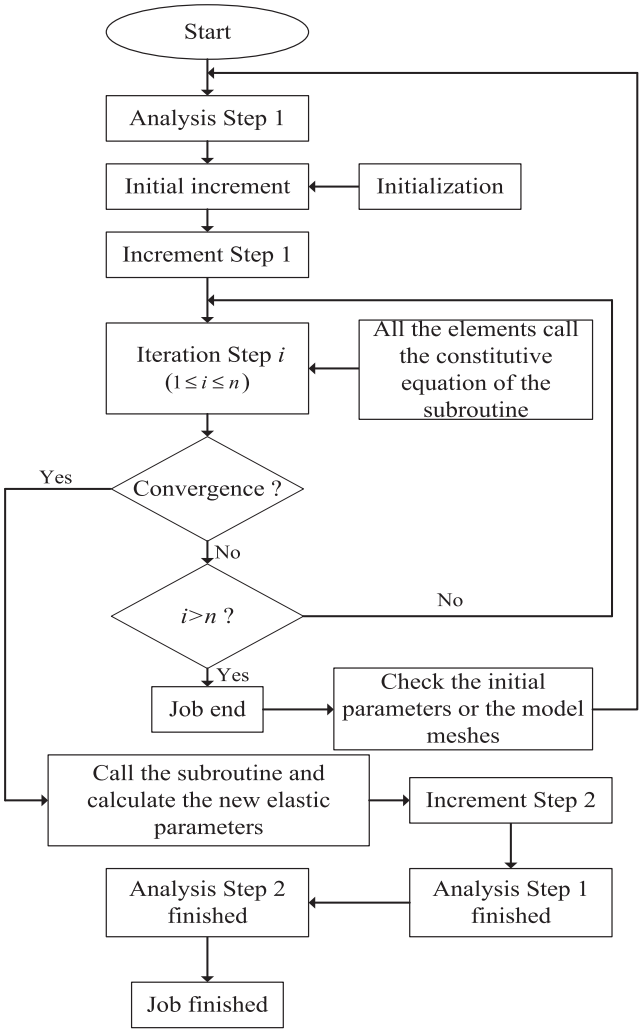

Fig. 1. Flow chart of the subroutine calculation process.

direction of maximum principal stress, and embedding Eq. (7) into the subroutine.

2.3. Model verification

To demonstrate the capability of the improved constitutive model, a conventional triaxial compression test was simulated. The equivalent elastic modulus and Poisson's ratio of the rock are 600 − 800 MPa and 0.2 − 0.3, respectively. The cohesion and friction angle of the rock matrix and soft interface are (2 MPa, 30°) and (1 MPa, 20°), respectively. Fig. 2 shows that α is the dip angle between the maximum principle stress and the interfaces in Jaeger's theory, while θ is the inclination angle between the interfaces and the horizontal plane ($\alpha = \frac{\pi}{2} - \theta$).

Fig. 3 illustrates the results for compressive strength under triaxial compression as the dip angle varies. Clearly, the compressive strength was significantly affected by the dip angle of soft interfaces within the range of 30°–80° and tended to minimize when the dip angle ranged from 50° to 60°. The compressive strength remained unvaried when the dip angle was beyond the range of 30°–80°. The numerical solution matches well with the analytic solution in Jaeger's theory for estimating the strength of anisotropic rock masses (Fig. 3). Therefore, the improved model can simulate the anisotropic characteristics of the layered rock mass.

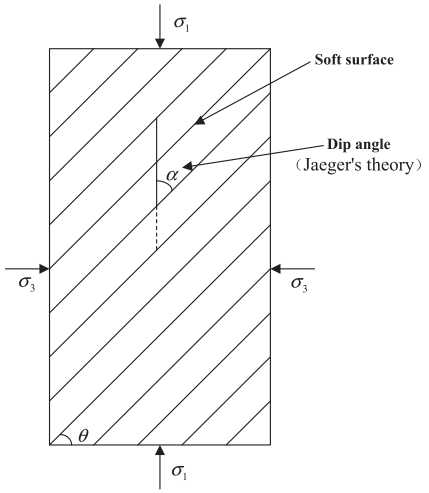

Fig. 2. The layered rock mass under triaxial compressive loading.

3. The equivalent simulation method for the bolted rock mass

3.1. Configuration of the numerical study

For different excavation shapes and support patterns of rock bolts (including bolt diameter ϕ, bolt spacing D and bolt length L), the effect of reinforcement on mechanical behavior of the bolted layered rock masses are different (Yang, 2004). To investigate the influence of bolt support patterns on the reinforcement effect for the surrounding rock masses (The zone which is three times to five times of the tunnel diameter) and variation of the equivalent parameter, a numerical model of tunnel excavation was established. The friction angle φ was taken as the equivalent parameter to simulate the bolted layered rock mass, which was changed in the surrounding rock masses. The developed constitutive model of the layered rock mass was adopted for the numerical simulation.

The numerical model size is 60 m × 60 m; the tunnel diameter is 10 m; the buried depth of the tunnel is 100 m; and the cohesion and friction angle of the weak interlayer plane are 0.065 MPa, 25°, correspondingly. The angle of the jointed plane is 30°. It assumes that the numerical model is under isotropic stress field of 4MPa along the X and Y directions of the model's boundary, and the bottom constraints of the model are fixed. Fig. 4 shows the model after the mesh and constraints. During the simulation of tunnel excavation, the loads are not released suddenly after the tunnel excavated. First, the initial stress balance was established. It assumed that 85% of the load was released after the tunnel excavated. The rock bolts withstood 5% loads for the initial support, and then shared 10% loads with the lining (Chen et al., 2010). The main effect of the rock bolts is controlling the deformation and changing the stress state of the surrounding rock mass. The bar element and beam element can both achieve this effect. In order to simplify the numerical model, the bar element was adopted for rock bolt in this section. The rock bolts were arranged perpendicular to the tunnel cycle. The beam elements were used to simulate the lining, and the thickness of the lining (d) equals 0.4 m. Table 1 lists the mechanical parameters of the bolt and lining.

The elastic modulus and Poisson's ratio of the rock mass are $E_1 = 3.779$ GPa, $E_2 = 2.439$ GPa and $\nu_1 = 0.254$, $\nu_2 = 0.180$. The shear modulus G_2 and weight density of the rock mass are 1.085 GPa and 23 kN·m^{-3}, respectively. The cohesion and internal friction angle of the rock mass are 0.65 MPa, 35°, respectively. E_1,ν_1,E_2,ν_2 and G_2 are the five independent elastic constants of the layered rock mass. E_1 and ν_1 are the elastic modulus and Poisson's ratio in the direction parallel to the bedding surface of the layered rock mass, and E_2, ν_2 and G_2 are the elastic modulus, Poisson's ratio and shear modulus in the direction

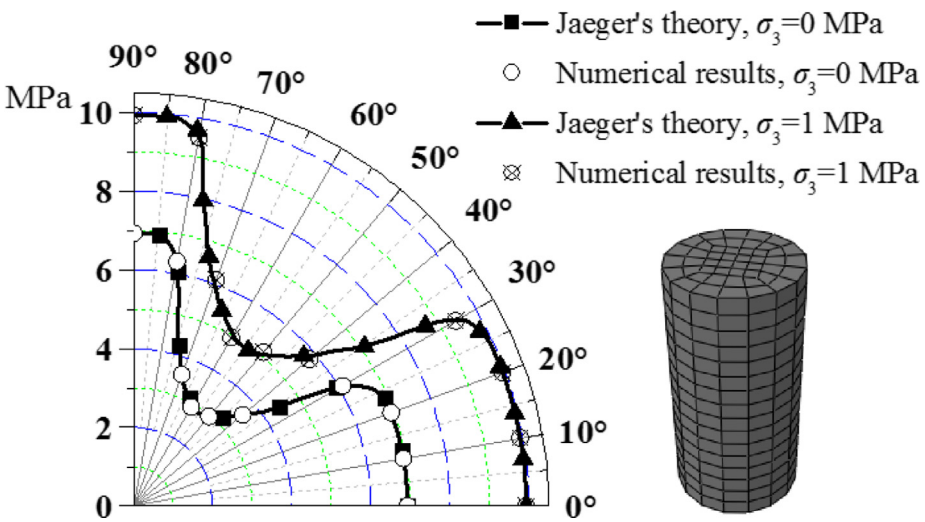

Fig. 3. The relationship between compressive strength and the dip angle (α) of layered rock mass.

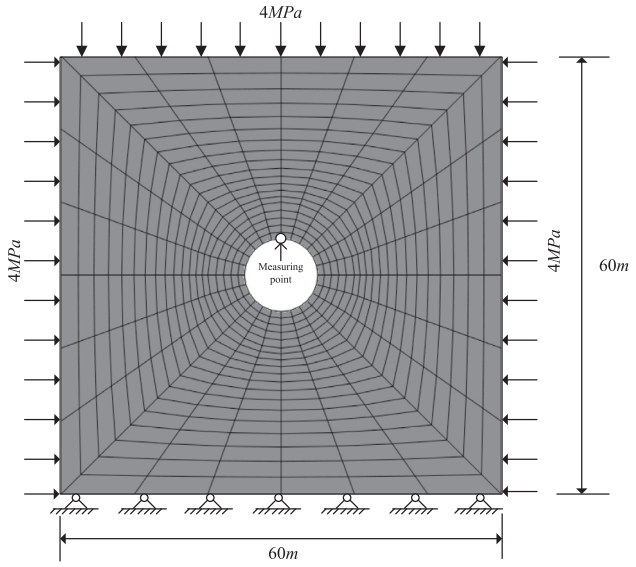

Fig. 4. Numerical model.

Table 1
The mechanical parameters of bolts and lining in the simulation.

Parameters	Lining	Bolt
Elastic modulus E(GPa)	28	210
Poisson's ratio μ	0.27	0.30
Density ρ(kN·m^{-3})	2500	7800

perpendicular to the bedding surface of the layered rock mass.

Twenty-eight numerical cases are designed in Table 2. Cases 2 to 28 are designed to explore the influence of bolt diameter ϕ, bolt spacing D and bolt length L on the reinforcement effect of the bolts. Fig. 5 shows the schematic view of the bolt support for case 2. The vertical displacement of the lining dome is selected for comparison. Numerical case 1 is the tunnel excavation without bolts installed, but just lining supported. Except for numerical case 1, the equivalent parameter φ of the bolted rock mass is adjusted for the numerical simulation without bolts installed, which should guarantee that the vertical displacement of the lining dome stays the same with the result of each case. Therefore, the equivalent parameter φ of the bolted rock mass can be obtained for each case.

Table 2
Input parameters of the bolting pattern in the numerical model.

Numerical case	Tunnel diameter R(m)	Bolt length L(m)	Bolt spacing D(m)	Bolt diameter ϕ(m)
1	10	0	0	0
2	10	2	1.3	25
3	10	2	1.3	28
4	10	2	1.3	32
5	10	2	2.5	25
6	10	2	2.5	28
7	10	2	2.5	32
8	10	2	3.8	25
9	10	2	3.8	28
10	10	2	3.8	32
11	10	3	1.3	25
12	10	3	1.3	28
13	10	3	1.3	32
14	10	3	2.5	25
15	10	3	2.5	28
16	10	3	2.5	32
17	10	3	3.8	25
18	10	3	3.8	28
19	10	3	3.8	32
20	10	5	1.3	25
21	10	5	1.3	28
22	10	5	1.3	32
23	10	5	2.5	25
24	10	5	2.5	28
25	10	5	2.5	32
26	10	5	3.8	25
27	10	5	3.8	28
28	10	5	3.8	32

3.2. Numerical results

Table 3 shows the vertical displacement of the tunnel lining dome obtained by different numerical cases. All numerical results were compared with the result acquired by numerical case 1, i.e., tunnel excavation without bolts installed. Table 4, and Figs. 6 and 7 were obtained from the results in Table 3. It is found that: The bolts can control about 8% displacement of the surrounding rock masses under the simulated geological conditions. Increasing the bolt length can effectively decrease the vertical displacement of the lining dome when the diameter and spacing of bolts are unchanged. The increase in the bolt spacing will weaken the reinforcement performance when the diameter and length of bolts are unchanged. Increasing the bolt diameter can also effectively reduce the vertical displacement of the lining dome when the length and spacing of bolts are unchanged. The effect of bolt spacing, diameter and length on limiting the vertical displacement

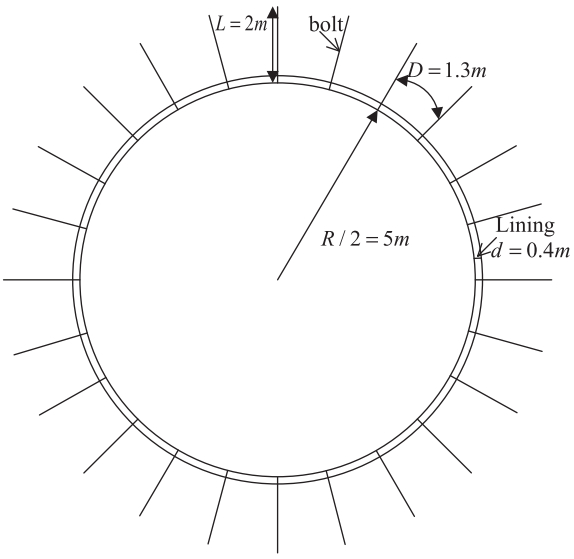

Fig. 5. The bolting pattern of numerical case 2.

Table 3
Results of the 28 numerical cases.

Numerical case			s(mm)	s_d(%)	φ(°)	φ_I(%)
Without bolts installed			19.14	0	35	0
L = 2m	D = 1.3m	ϕ25	18.12	5.33	38.84	5.26
		ϕ28	18.10	5.43	36.92	5.49
		ϕ32	18.09	5.49	36.97	5.63
	D = 2.5m	ϕ25	18.34	4.18	36.48	4.23
		ϕ28	18.31	4.34	36.53	4.37
		ϕ32	18.27	4.55	36.64	4.69
	D = 3.8m	ϕ25	18.68	2.40	35.80	2.29
		ϕ28	18.64	2.61	35.96	2.74
		ϕ32	18.56	3.03	36.05	3.00
L = 3m	D = 1.3m	ϕ25	17.72	7.42	37.60	7.43
		ϕ28	17.64	7.84	37.75	7.86
		ϕ32	17.56	8.25	37.90	8.29
	D = 2.5m	ϕ25	17.86	6.69	37.35	6.71
		ϕ28	17.78	7.11	37.49	7.11
		ϕ32	17.71	7.47	37.62	7.49
	D = 3.8m	ϕ25	18.22	4.81	36.69	4.83
		ϕ28	18.05	5.70	37.00	5.71
		ϕ32	17.89	6.53	37.30	6.57
L = 5m	D = 1.3m	ϕ25	17.16	10.34	38.70	10.57
		ϕ28	17.06	10.87	38.82	10.92
		ϕ32	17.00	11.18	38.92	11.20
	D = 2.5m	ϕ25	17.30	9.61	38.38	9.66
		ϕ28	17.24	9.93	38.48	9.94
		ϕ32	17.19	10.19	38.58	10.23
	D = 3.8m	ϕ25	17.56	8.25	37.90	8.29
		ϕ28	17.47	8.73	38.10	8.86
		ϕ32	17.39	9.14	38.22	9.20

Note: s is the vertical displacement of lining dome; s_d is the decreased percentage of the vertical displacement of lining dome; φ_I is the increased percentage of the equivalent parameter φ.

of the lining dome is different. The sensitivity of their influence on controlling the deformation is: bolt length > bolt spacing > bolt diameter. The variation of the equivalent parameter is basically same as the variation of vertical displacement of the lining dome.

Figs. 6 and 7 indicates that when the ratio of bolt length to tunnel diameter (L/R) is unvaried, the percentage of the vertical displacement reduction increases as the ratio of bolt diameter to bolt spacing (ϕ/D) increases. When ratio of bolt diameter to bolt spacing (ϕ/D) is unchanged, the percentage of vertical displacement reduction increases if the ratio of bolt length to tunnel diameter (L/R) increases. The increase of the equivalent parameter φ percentage has the same trend as the percentage of vertical displacement reduction (Table 3). Therefore, the improved value of the equivalent parameter φ is related to bolt diameter ϕ, bolt length L, bolt spacing D and tunnel excavation diameter R. The ratio of bolt diameter to bolt spacing (ϕ/D), and the ratio of bolt length to tunnel diameter (L/R) are the two influencing factors for the equivalent parameter φ.

3.3. The equivalent simulation method

The two factors L/R and ϕ/D both have an influence on the improved value of equivalent parameter φ, but the influence degree of the two factors is different. How to reasonably determine the comprehensive effect of the two factors is becoming the key problem. The coefficient of each influence factor is determined by subjective speculation for solving these problems in many other cases. It can objectively reflect the actual situation to some extent in the special issue. Its evaluation results also have great reference value, but its subjective color is relatively strong. Therefore, it will deviate from the objective reality in some cases. Then, the results in new problems are misjudged. Thus, mathematic methods were used to determine the coefficient of the two influence factors in this paper. Although mathematic methods also have a certain subjective color, they can make the final results objective and reliable, and meet the actual situation because of rigorous logic and strong mathematic processing ability. The multiple linear regression analysis method was used for fitting the formula of equivalent parameter φ with the two influence factors L/R and ϕ/D in this paper.

The powerfully mathematic and statistical analysis software SPSS is used for solving the multiple linear regression analysis problems and fitting the multiple linear regression equation. The increased percentage of the equivalent parameter $\varphi(\Delta\varphi/\varphi)$ is the dependent variable, and the two influence factors L/R and ϕ/D are independent variables. The numerical results are imported into the SPSS software, and Tables 5–9 and Fig. 8 show the analysis results.

The descriptive statistical results including the Average Value, Standard Deviation and Simple Number of the three variables in the regression analysis are shown in Table 5. The correlation coefficient and significance test for the six variables in the process of multiple linear regression analysis are given in Table 6. Table 7 reveals the fitting effect of the regression equation. The correlation coefficient of the model is 0.973, and the determination coefficient of the analysis model is 0.946, and the adjusted determination coefficient is 0.941, illustrating that the equation fit very well. The value of Durbin-Watson is 1.756, which is close to 2. So the analysis model cannot be considered as the autocorrelation model. The residual analysis and test results of the regression equation are shown in Table 8. The value of F and P from the regression equation are 209.886 and 0.000, respectively, reflecting that the regression equation is significant. The non-normalized estimation coefficient, the standardized estimation coefficient values, the significance of the statistical test results and the covariance diagnostic variance factor of the regression equation are shown in Table 9. Fig. 8 shows the 27 observed values are all between −2 and +2, demonstrating that the equation fitting is good.

Finally, the regression equation for the increased percentage of the equivalent parameter $\varphi(\Delta\varphi/\varphi)$ with the two factors L/R and ϕ/D is obtained through multiple linear regression analysis, and it can be written as:

$$\Delta\varphi/\varphi = 0.184(L/R) + 1.495(\phi/D) - 0.012 \quad (8)$$

Eq. (8) can be used for calculating the equivalent parameter φ, which can be adopted for simulating bolted layered rock masses in tunnel engineering without bolts installed. Therefore, Eq. (8) can be defined as the equivalent simulation method for bolted layered rock masses.

Table 4
Comparison of the performance of the bolt with varying support parameters.

Numerical case			s(mm)	s_d(%)	Numerical case			s(mm)	s_d(%)
Without bolts installed			19.14	0	Without bolts installed			19.14	0
L = 2	ϕ25	D1.3	18.12	5.33	ϕ25	D1.3	L = 2	18.12	5.33
		D2.5	18.34	4.18			L = 3	17.72	7.42
		D3.8	18.68	2.40			L = 5	17.16	10.34
	ϕ28	D1.3	18.10	5.43		D2.5	L = 2	18.34	4.18
		D2.5	18.31	4.34			L = 3	17.86	6.69
		D3.8	18.64	2.61			L = 5	17.30	9.61
	ϕ32	D1.3	18.09	5.49		D3.8	L = 2	18.68	2.40
		D2.5	18.27	4.55			L = 3	17.86	6.69
		D3.8	18.56	3.03			L = 5	17.30	9.61
L = 3	ϕ25	D1.3	17.72	7.42	ϕ28	D1.3	L = 2	18.10	5.43
		D2.5	17.86	6.69			L = 3	17.64	7.84
		D3.8	18.22	4.81			L = 5	17.06	10.87
	ϕ28	D1.3	17.64	7.84		D2.5	L = 2	18.31	4.34
		D2.5	17.78	7.11			L = 3	17.78	7.11
		D3.8	18.05	5.70			L = 5	17.24	9.93
	ϕ32	D1.3	17.56	8.25		D3.8	L = 2	18.31	4.34
		D2.5	17.71	7.47			L = 3	18.05	5.70
		D3.8	17.89	6.53			L = 5	17.47	8.73
L = 5	ϕ25	D1.3	17.16	10.34	ϕ32	D1.3	L = 2	18.09	5.49
		D2.5	17.30	9.61			L = 3	17.56	8.25
		D3.8	17.56	8.25			L = 5	17.00	11.18
	ϕ28	D1.3	17.06	10.87		D2.5	L = 2	18.27	4.55
		D2.5	17.24	9.93			L = 3	17.71	7.47
		D3.8	17.47	8.73			L = 5	17.19	10.19
	ϕ32	D1.3	17.00	11.18		D3.8	L = 2	18.56	3.03
		D2.5	17.19	10.19			L = 3	17.89	6.53
		D3.8	17.39	9.14			L = 5	17.39	9.14

Note: s is the vertical displacement of lining dome; s_d is the decreased percentage of the vertical displacement of lining dome.

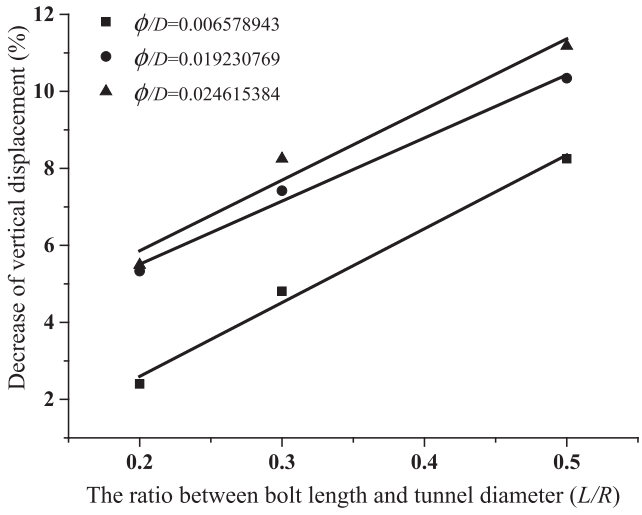

Fig. 6. The effect of L/R on the decrease of the vertical displacement.

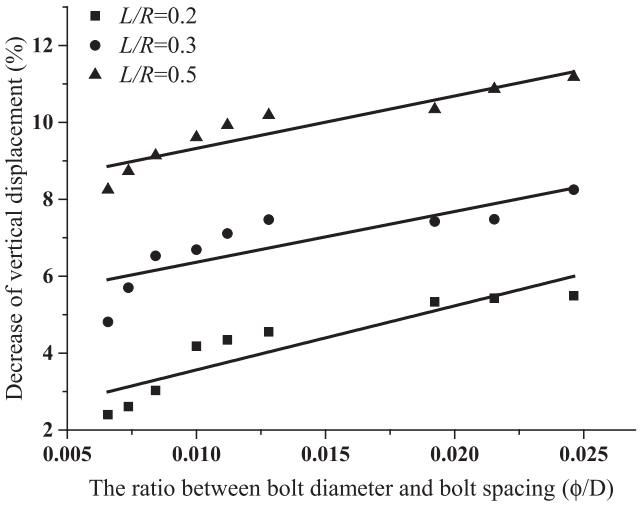

Fig. 7. The effect of ϕ/D on the decrease of the vertical displacement.

3.4. Discussions

The main difficulty in this study is the selection of the equivalent parameter. However, there is no commonly accepted notion on the improved mechanical parameters of the bolted rock mass. To determine the improved parameters, numerical calculations were conducted based on the numerical model in Section 3.1. The vertical displacement and horizontal displacement of the arch foot were selected for comparison. The results for tunnels with bolts installed are calculated by the numerical case 20 in Section 3.1. The improved jointed material model was adopted for the numerical simulation. Tables 10 and 11 show the numerical results.

The improved parameters of the surrounding rock masses can equivalently simulate the reinforcement effect of the rock bolts, but the improved value of the parameter is different (Tables 10 and 11). The values of cohesion and internal friction angle were improved separately as 1.7 times and 1.1 times the initial value of the surrounding rock mass. It can also be found that the degree of sensitivity for simulating the rock bolt reinforcement through improving the parameter of the surrounding rock mass is different. The most sensitive parameter is the

Table 5
Descriptive statistics of the three variables.

Variable	Average	Standard deviation	N
$\Delta\varphi/\varphi$	0.0698	0.02593	27
L/R	0.3333	0.12710	27
ϕ/D	0.0135	0.00636	27

Table 6
Correlation of the three variables.

Variable		$\Delta\varphi/\varphi$	L/R	ϕ/D
Pearson correlation	$\Delta\varphi/\varphi$	1.000	0.901	0.367
	L/R	0.901	1.000	0.000
	ϕ/D	0.367	0.000	1.000

Table 7
Collection of the analysis.

Model	R	R^2	Adjustment R^2	Standard estimation deviation	Durbin-Watson
1	0.973	0.946	0.941	0.00628	1.756

Table 8
Analysis of the dependent variable.

Model		Square sum	DF	Mean square	F	P value
1	Regression	0.017	2	0.008	209.886	0.000
	Residual	0.001	24	0.000		
	Total	0.017	26			

internal friction angle, followed by cohesion (Fig. 9). This result is consistent with the findings in Cai et al. (2004). However, the improved magnitude of the parameters is different. The internal friction angle needs to be improved 1.7 times over the initial value by Cai et al. (2004). The main reason is that the surrounding rock masses is assumed to be isotropic material (Cai et al., 2004). The improved cohesion and internal friction angle can both simulate the bolted rock mass, and the difference is the improved value.

The equivalent simulation method for bolted rock masses was also studied through FLAC3D modeling by Yang (2004), in which the formula of the improved parameter was proposed as $\Delta C/C = 0.0229\ln(L/R) + 0.0486\ln(\phi/D) + 0.3100$. The improved parameter by Yang (2004) was cohesion, and the two influential factors were the same as Eq. (8) in this paper. The form of the two factors given by Yang (2004) is logarithmic, which differs from the form of Eq. (8). Calculation of the improved parameters using Eq. (8) is easier. More accurate determination of improved parameters such as cohesion needs to be further investigated for the layered rock mass.

4. Engineering validation

4.1. Engineering project overview

4.1.1. Huashan road project overview

The total length of the project is 15.225km. Huashan Road goes through the Jiufeng Mountains, including Baogai Mountain, Boyu Feng and Changshan Mountain. The Baogai Mountain tunnel and Changshan Mountain tunnel are excavated along the Road. The stake number of the Baogai Mountain tunnel entrance is K0 + 963, and the exit is K1 + 550. The total length of the Baogai Mountain tunnel is 587 m, and it is a medium-long tunnel. A pedestrian cross-channel is set in the middle of the tunnel with better conditions of the surrounding rock masses. The profile of Baogai Mountain tunnel is unidirectional slope, and it is lower from south to north gradually. The angle of the slope is −0.5%. The paring-bamboo port parts are set at 22 m of the tunnel entrance and 40 m of the tunnel exit respectively. The elevation of Baogai Mountain and Boyu Feng above the tunnel are approximately 137 m and 117 m. The maximum depth of the tunnel is approximately 63.5 m, and the depth of the tunnel in the valley between Baogai Mountain and Boyu Feng is approximately 6.5 m.

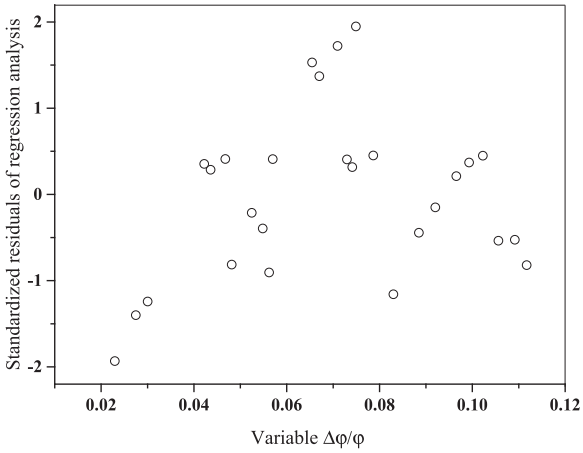

Fig. 8. Standardized residuals scatter plot.

Table 10
Equivalent simulation results by improving the cohesion of surrounding rock mass.

Improved parameter	Displacement of lining (mm)	
	Vertical displacement of dome	Horizontal displacement of arch foot
With bolts installed	17.16	5.02
Without bolts installed	19.14	7.76
1.1c	18.18	6.52
1.2c	17.86	6.24
1.3c	17.61	6.06
1.4c	17.42	5.88
1.5c	17.30	5.72
1.6c	17.23	5.64
1.7c	17.16	5.56
1.8c	17.09	5.48
1.9c	17.02	5.40
2.0c	16.95	5.32

4.1.2. Hydrogeologic conditions

Baogai Mountain tunnel is located at a structural denudation and low mountain landform area, and the elevation of Baogai Mountain and Boyu Feng above the tunnel are approximately 137 m and 117 m. There is a V-shaped gully between Baogai Mountain and Boyu Feng, and it is the main gully of the field area. The west ern gully is small and narrow, and then it gradually widens to the east. There are mountain peaks,

Table 9
The coefficient of the model analysis.

Model	Un-standard coefficient		Standard coefficient	t	Sig	Correlation			Co linearity statistics	
	B	Standard deviation				Zero-order	Partial	Part	Tolerance	VI-F
Constant	0.012	0.004		−2.689	0.013					
L/R	0.184	0.010	0.901	18.98	0.000	0.901	0.968	0.901	1.0	1.0
ϕ/D	1.495	0.194	0.367	7.723	0.000	0.367	0.844	0.367	1.0	1.0

Table 11
Equivalent simulation results by improving the friction angle of surrounding rock mass.

Improved parameter	Displacement of lining (mm)	
	Vertical displacement of dome	Horizontal displacement of arch foot
With bolts installed	17.16	5.02
Without bolts installed	19.14	7.76
1.1φ	17.09	5.96
1.2φ	16.73	5.22
1.3φ	16.42	4.80
1.4φ	16.19	4.68
1.5φ	16.03	4.56
1.6φ	16.00	4.50
1.7φ	16.08	4.64
1.8φ	16.18	4.70
1.9φ	16.28	4.80
2.0φ	16.28	4.82

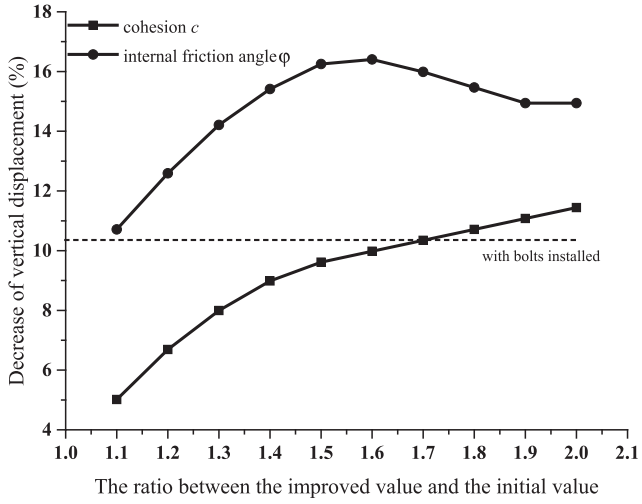

Fig. 9. The sensitivity of the improved parameter to decrease the vertical displacement of lining dome.

ridges, watersheds and gullies in the tunnel crossing area, and the elevation of the tunnel cross section is 78.06–90.36 m. The tunnel entrance is located at the foot of the southern slope of Baogai Mountain, where the natural slope angle is approximately 16°–25°, and the tunnel exit is located at the north side of Boyu Feng, where the natural slope angle is 15°–20°.

According to the geologically surveyed engineering results, the overall trend of the mountain is basically the same as the tectonic line direction. The Silurian to Carbonaceous system strata in the area form a single monoclinic structure. The overall trend of the geology is

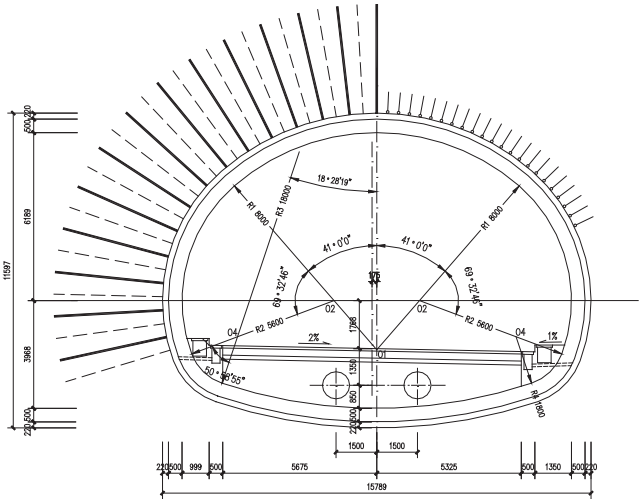

Fig. 11. Composite lining of IV surrounding rock design schematic (1:100).

northwestward to the west (NWW), it is inclined to the northeast approximately 20°, and the average inclination angle is approximately 40°. The faults in this area are not developed, and the only reverse fault (F) of Wangjia Dian which is approximately 1500 m long, passes through the project area. The trend of the fault is basically same as the rock layers. It is a one-step fault in the NWW direction. The project area is located at the eastern section of the fault, and the width of the fault zone is not detailed because of the quaternary stratum coverage. Based on the drilling data and geological mapping results, the Silurian-Carboniferous system strata repeats from south to north because of the fault. The strata is a reverse fault, and its inclination is approximately 50°. The strength of quartz sandstone in the Wutong group of Baogai Mountain tunnel is high, and the main deformation characteristics are brittle.

4.1.3. Section information of left line K1 + 050 of Baogai Mountain tunnel

The left line and right line of Baogai Mountain tunnel were excavated for the K0 + 980–K1 + 053. The arc-excavation and core soil preservation method was used for the tunnel excavation, and the left and right lines of the tunnel excavation were staggered. According to geological survey data, the surrounding rock mass of the K1 + 050 section of Baogai Mountain tunnel was classified as IV. The IV support was adopted for the K1 + 050 section during the process of excavation according to the design requirements. The overburden of the excavated part was shallow, and the rock mass was seriously weathered. Therefore, the integrity and strength of the rock mass was poor. Fig. 10 shows the joints of the surrounding rock mass of section K1 + 050. The problems we faced during construction were: (1) the deformation of the tunnel dome was large; (2) the blocks were broken and came down from the tunnel dome; and (3) particularly, the vault of the left line section K1 + 050 of the tunnel was damaged seriously.

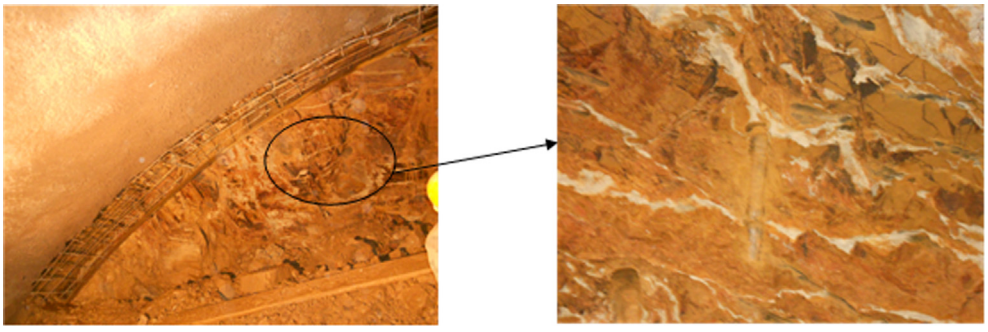

Fig. 10. The joints of surrounding rock mass.

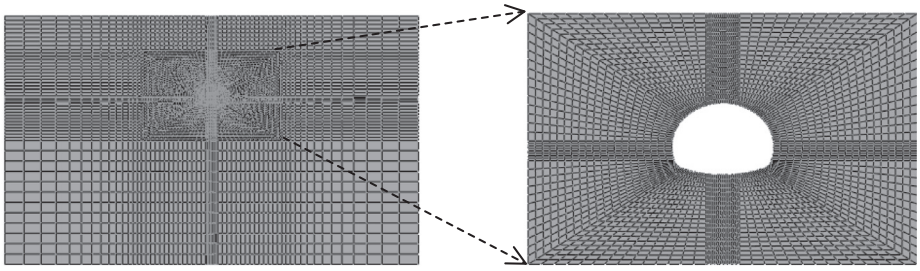

(a) Numerical calculation model (b) Surrounding rock mass

Fig. 12. Numerical model of Section K1 + 050.

Table12
The mechanical parameters of the numerical model section K1 + 050.

Material	Elastic modulus E(GPa)		Poisson's ratio μ		Cohesion c(MPa)	Shear modulus G_2(GPa)	Friction angle φ(°)	Density ρ(kN·m^{-3})
Rock mass	E_1	E_2	μ_1	μ_2	0.6	1.24	40	2500
	4	0.4	0.30	0.35				
Lining	30		0.25					2500
Bolt	210		0.30					7800

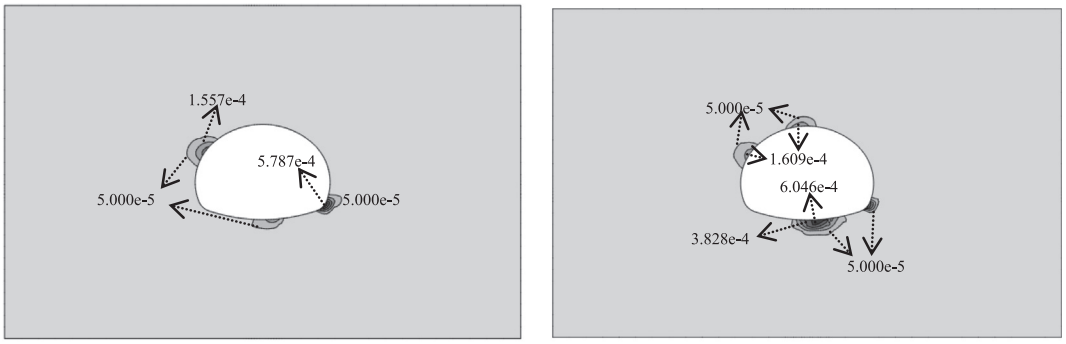

(a) plastic zone of configuration 1 (b) plastic zone of configuration 2

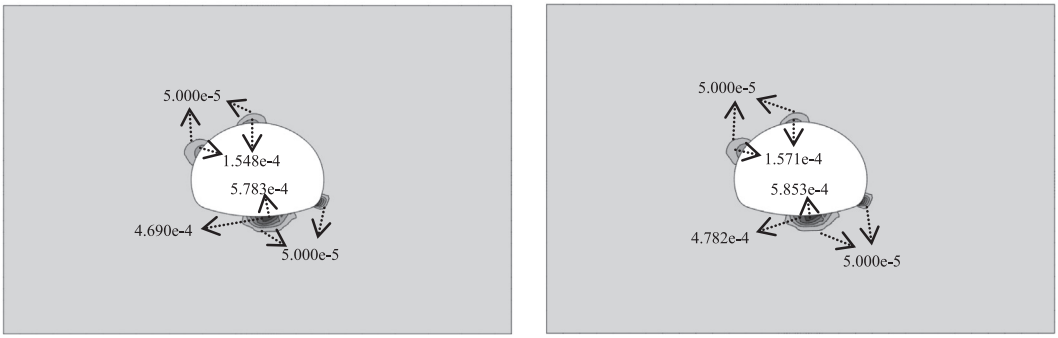

(c) plastic zone of configuration 3 (d) plastic zone of configuration 4

Fig. 13. Equivalent plastic zone of surrounding rock masses.

The Baogai Mountain tunnel left line section K1 + 050 of Huashan Road was selected for the numerical simulation in this paper, and the composite lining form was adopted. The IV surrounding rock mass support form of Baogai Mountain tunnel is shown in Fig. 11. The observation data of the left line of section K1 + 050 indicated that the settlement of the tunnel top arch was 18.72 mm, and the settlement of the lining top arch was 18.68 mm. The deformation of the tunnel top arch was downward, and the deformation of the tunnel sidewall was oblique up. In addition, the floor of the tunnel was upward slightly. The damaged area of section K1 + 050 was large, especially the deformation and the fractured area of the surrounding rock mass of the tunnel top arch were large, and the stability of the surrounding rock mass was poor. The damage area of the section K1 + 050 emerged because of the collapsed impact of the section K1 + 053 nearby. The fracture area did not exist at the sidewall, but the stress concentration should be noted.

4.2. Numerical model and calculation configurations

4.2.1. Numerical model

According to the geological data from Baogai Mountain tunnel, a detailed two-dimensional numerical model of the tunnel section K1 + 050 was established by the large-scale finite element analysis

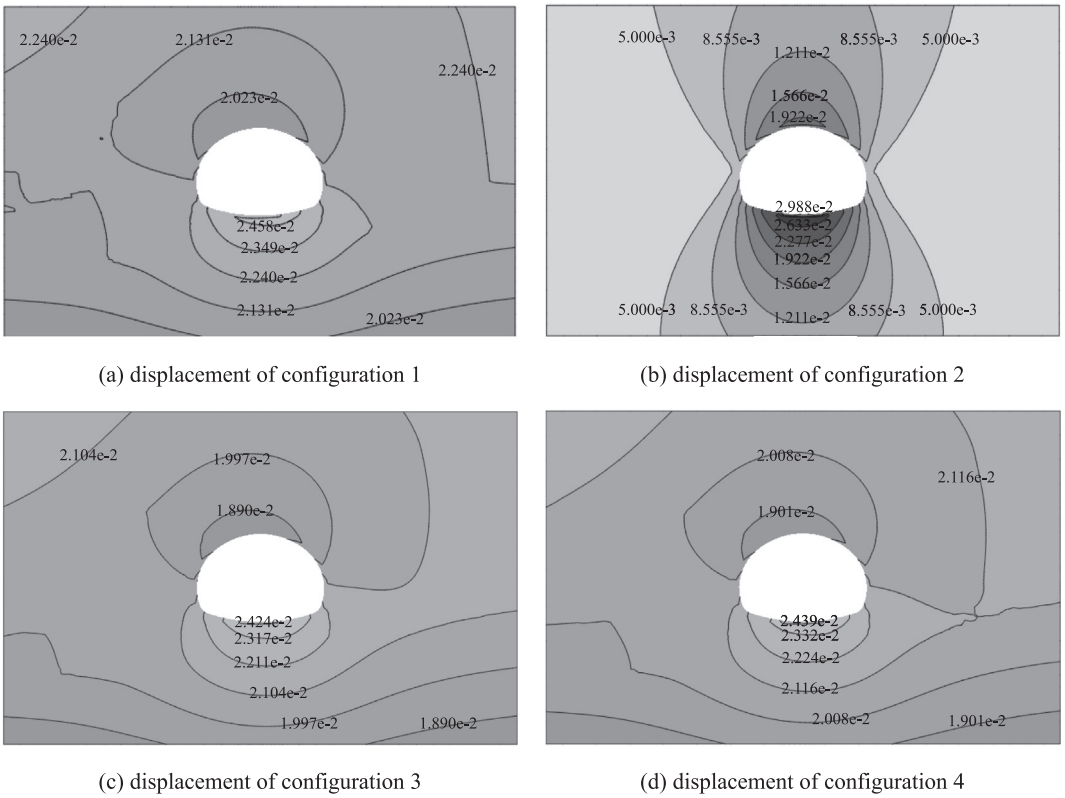

(a) displacement of configuration 1 (b) displacement of configuration 2

(c) displacement of configuration 3 (d) displacement of configuration 4

Fig. 14. Displacement of the surrounding rock masses (unit: m).

Table 13
Vertical displacement of different configurations.

Configurations	Configuration 1	Configuration 2	Configuration 3	Configuration 4	Monitoring data
Displacement of tunnel dome (mm)	19.27	19.87	18.52	18.67	18.72
Displacement of lining dome (mm)	19.03	18.82	18.28	18.41	18.68

software ABAQUS. The lengths of the X and Y directions of the model were 161.48 m and 97.42 m, respectively; and the top surface of the model was free. The left and right sides of the model were imposed by horizontal constraints, and the bottom boundary of the model was fixed. The lateral pressure coefficient was 0.77. The numerical model consisted of four parts, including surrounding rock masses, excavated rock masses, concrete lining and bolts. The finite element mesh is shown in Fig. 12, and meshes of the model were partitioned with structured quadrilateral elements. The numerical model was divided into 8383 nodes and 8256 cells. The element type of the rock mass was CPE4; the element type of the lining was CPE4I, and the thickness of lining was 0.6 m. The diameter and length of the bolts were 25 mm and 4.5 m respectively, and the beam element was adopted for bolt simulation, with a bolt range spacing of 1.1 m. The 28 bolts were arranged around the tunnel cycle. The stress field generated by gravity was only taken into consideration in the process of numerical simulation. First, the initial stress balance was established, then the method of modulus attenuation was adopted for simulating the effect of stress release in the process of the tunnel excavation. The material parameters of the model are shown in Table 12.

4.2.2. Numerical verification of the proposed equivalent simulation method

Four numerical configurations were adopted to simulate the deformation of section K1 + 050. The plastic zone, deformation and stress of the surrounding rock masses in the process of tunnel excavation were compared and analyzed. The four calculation configurations were:

(1) Configuration 1: The jointed material model in ABAQUS;
(2) Configuration 2: The proposed anisotropic constitutive model of layered rock masses without bolts installed;
(3) Configuration 3: The proposed anisotropic constitutive model of layered rock masses with bolts installed;
(4) Configuration 4: The established equivalent reinforcement formula (8) was adopted for calculating the equivalent anchoring parameter. Then, the deformation of section K1 + 050 of Baogai Mountain tunnel was equivalently simulated by the proposed anisotropic constitutive model. The equivalent parameter was calculated by assuming that section K1 + 050 was a circular tunnel, and its diameter was 10m because it is composed of several arcs. The percentage of the equivalent parameter was increased 10.48% as calculated by Eq. (8).

4.3. Numerical results

4.3.1. Plastic zone of the surrounding rock masses

Fig. 13 shows the plastic zone of the surrounding rock mass simulated by the four numerical configurations. The surrounding rock mass in configuration 1 was assumed to be isotropic material, however, the surrounding rock mass in the other three conditions was assumed to be anisotropic material. Fig. 13(b) and (c) showed that the plastic zones of the surrounding rock masses were similar and anti-symmetrically distributed. The plastic zone emerged in the upper left and lower right area of the tunnel. From the plastic zone in Fig. 13(a), we could find that the top arch of the tunnel was undamaged, however it was

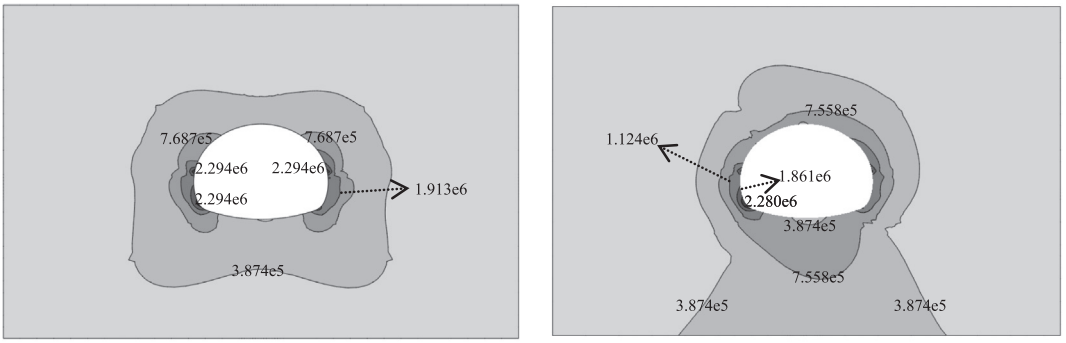

(a) Mises stress of configuration 1

(b) Mises stress of configuration 2

(c) Mises stress of configuration 3

(d) Mises stress of configuration 4

Fig. 15. Von-Mises stress of surrounding rock masses (unit: Pa).

different from the other three configurations. The damaged area of the tunnel top arch in Fig. 13(b)–(d) was similar to the actual situation during the construction process of the section K1 + 050. It demonstrated that the jointed material model in ABAQUS adopted in configuration 1 cannot accurately reflect the damaged area of the section K1 + 050 during the tunnel excavation. However, the developed model in this paper adopted in configuration 2 can reflect the deformation and destruction of the surrounding rock mass to some degree. It also found that the bottom of the tunnel was damaged in all conditions consistent with the actual situation of section K1 + 050. The main reason was that the stress was released during tunnel excavation. Therefore, the concrete grouting support should be carried out in time for the tunnel floor during the construction.

The plastic zone calculated for configuration 3 in Fig. 13(c) was compared with configuration 4 in Fig. 13(d). We found that the plastic zone in Fig. 13(c) was similar to the plastic zone in Fig. 13(d), while the plastic zone in Fig. 13(d) was slighter larger than the plastic zone in Fig. 13(c). The plastic zone calculated for configuration 4 in Fig. 13(d) was consistent with the actual situation of section K1 + 050 in Baogai Mountain tunnel. It revealed that the equivalent anchoring method (Eq. (8)) could simulate the reinforcement effect of rock bolts. However, the equivalent anchoring method (Eq. (8)) was limited to certain geological conditions, and it was based on numerical calculation. The equivalent anchoring mechanism theory for anisotropic rock masses is extremely complicated, so it was not studied in this paper.

4.3.2. Deformation of the surrounding rock masses

The deformation of the rock masses surrounding section K1 + 050 were obtained by the four configurations. The displacement of the surrounding rock masses is shown in Fig. 14. According to the actual monitoring data for section K1 + 050, the displacement of the tunnel dome and the lining dome were 18.72mm and 18.68mm after the support was finished three days later. The dome displacement, the study subjects, monitoring data and numerical calculation data for the tunnel and lining are settled in Table 13.

Fig. 14(a) showed that distribution of the displacement cloud contour was symmetric when the surrounding rock mass was isotropic. In contrast, the displacement cloud contours were un-symmetric in Fig. 14(b)–(d) when the surrounding rock mass was anisotropic. It demonstrates that the developed model of layered rock masses in this paper is reasonable. The displacement of the surrounding rock masses in Fig. 14(a) was larger than the displacement in Fig. 14(b)–(d). The displacement in Fig. 14(c) had a slight difference with the displacement in Fig. 14(d). However, the values of displacements in Fig. 14(c) and (d) was close to each other.

The monitoring and the numerical calculation data of the tunnel dome and lining dome are shown in Table 13. We found that the displacement calculated by configurations 3 and 4 was close to the monitoring data. It revealed that the developed model of layered rock masses could simulate the process of the tunnel excavation and support. In addition, the equivalent anchoring method (Eq. (8)) could simulate the reinforcement effect of the rock bolts demonstrating that the proposed equivalent simulation method for bolted rock masses was reasonable.

4.3.3. Stress of the surrounding rock masses

Fig. 15 shows the Von-Mises stress of the surrounding rock masses calculated by four configurations. The Von-Mises stress contours were symmetric in Fig. 15(a), however the Von-Mises stress contours in Fig. 15(b)–(d) were un-symmetric and exhibited anisotropic characteristics. The stress concentration appeared at the left bottom corner and two middle sides of the tunnel after excavation in Fig. 15. This was consistent with the situation in the section K1 + 050 after the excavation. Therefore, we should especially pay attention to the stress of these three places for tunnel excavation, and avoid the appearance of large deformation and destruction at these three places.

The distribution of the Von-Mises contours in Fig. 15(b)–(d) were similar, but the stress in Fig. 15(c) was smaller than the stress in

Fig. 15(b) due to the installation of the rock bolts. The stress in Fig. 15(d) calculated by the equivalent numerical simulation method was close to the stress in Fig. 15(c). It demonstrated that the proposed equivalent anchoring method (Eq. (8)) was reasonable. The proposed method substantially simplifies the numerical process and the computational complexity. Therefore, the model can be employed to adequately represent the mechanical behavior of the bolted rock masses in practical engineering cases.

5. Conclusions

(1) The anisotropic constitutive model of layered rock masses was proposed in this paper, and the FORTRAN language was used for secondary development. Then the proposed model was numerically implemented in ABAQUS. The effectiveness and reliability of the proposed model was validated by numerical triaxial testing.
(2) Based on the proposed model, 28 numerical cases were prescribed for investigating the equivalent anchoring mechanism. We found the support parameters affecting the equivalent reinforcement effect were different for anisotropic layered rock masses. The order of their influence was: bolt length > bolt spacing > bolt diameter.
(3) The equivalent anchoring mechanism was analyzed through the multiple linear regression method, and the formula of equivalent parameter ($\Delta\varphi/\varphi$) between the two factors L/R and ϕ/D was obtained: $\Delta\varphi/\varphi = 0.184(L/R) + 1.495(\phi/D) - 0.012$. The applicability of the formula was showed by simulating an underground tunnelling case.
(4) A detailed two-dimensional numerical model of section K1 + 050 of the Baogai Mountain tunnel was established based on the geological investigations. The numerical results were compared with the monitoring data. The good agreement between numerical results and field observations shows the proposed simulation method is capable of simulating the mechanical behavior of the anisotropic rock masses with rockbolting.

Acknowledgements

The authors would like to appreciate the financial supports from projected (No. 51678066) supported by Natural Science Foundation of China; Project (No. 2014CB047100) supported by the National Key Basic Research and Development Program of China 973 Program; Project (No. 2015CFB194) supported by Natural Science Foundation of Hubei Province of China and the Fundamental Research Funds for the Central University (grant No. DUT17RC(3)032).

References

ABAQUS, Inc., 2012. Abaqus analysis user's manual, 23.5.1 Jointed material model.
Ahmad, F., Soroush, H., 2005. A theoretical approach for analysis of the interaction between grouted rockbolts and rock masses. Tunn. Undergr. Space Technol. 20, 333–343.
Amadei, B., 1996. Importance of anisotropy when estimating and measuring in situ stress in rock. Int. J. Rock Mech. Min. Sci. Geomech. Abstr. 33 (3), 293–325.
Amadei, B., Pan, E., 1992. Gravitational stress in anisotropic rock masses with inclined strata. Int. J. Rock Mech. Min. Sci. Geomech. Abstr. 29 (3), 225–236.
Bernaud, D., Samir, M., de Buhan, P., et al., 2009. A numerical approach for design of bolt-supported tunnels regarded as homogenized structures. Tunn. Undergr. Space Technol. 29, 533–546.
Bobet, A., Einstein, H.H., 2011. Tunnel reinforcement with rockbolts. Tunn. Undergr. Space Technol. 26, 100–123.
Cai, X.L., Zhao, D.A., 2004. Probe into simulation of the bolt function by increasing geometrical parameters in tunnel calculation. J. Lanzhou Jiaotong Univ.: Nat. Sci. 23 (1), 10–14 (in Chinese).
Cai, Y., Esaki, T., Jiang, Y.J., 2004. An analytical model to predict axial load in grouted rock bolt for soft rock tunnelling. Tunn. Underground Space Technol. 19, 607–618.
Cai, Y., Jiang, Y.J., Djamaluddin, I., 2015. An analytical model considering interaction behavior of grouted rock bolts for convergence–confinement method in tunneling design. Int. J. Rock Mech. Min. Sci. 76, 112–126.
Chen, C.S., Pan, E., Amadei, B., 1998. Determination of deformability and tensile strength of anisotropic rock using Brazilian tests. Int. J. Rock Mech. Min. Sci. 35 (1), 43–61.
Chen, D.F., Feng, X.T., Xu, D.P., 2015. An equivalent numerical method for evaluating the reinforcing effectiveness of grouted bolts. Rock Soil Mech. 36 (4), 1195–1204 (in Chinese).
Chen, L., Tan, Y.L., Zang, C.W., et al., 2014. Test study of mechanical properties and failure characteristics of anchored rock. Rock Soil Mech. 35 (2), 413–422 (in Chinese).
Chen, W.Z., Wu, G.J., Jia, S.P., 2010. Application of ABAQUS in Tunnel and Underground Engineering. China Water and Power Press (in Chinese).
Chen, W.Z., Zhu, W.S., 2001. Solidification effect of jointed rock mass and its application to the slope engineering. Site Invest. Sci. Technol. 1, 3–6 (in Chinese).
Colak, K., Unlu, T., 2004. Effect of transverse anisotropy on the Hoek-Brown strength parameter 'm_i' for intact rocks. Int. J. Rock Mech. Min. Sci. 41, 1045–1052.
Donath, F.A., 1961. Experimental study of shear failure in anisotropic rocks. Geol. Soc. Am. Bull. 72 (6), 985–989.
Ghadimi, M., Shahriar, K., Jalalifar, H., 2015. A new analytical solution for the displacement of fully grouted rock boltin rock joints and experimental and numerical verifications. Tunn. Undergr. Space Technol. 50, 143–151.
Ghazvinian, A., Vaneghi, R.G., Hadei, M.R., Azinfar, M.J., 2013. Shear behavior of inherently anisotropic rocks. Int. J. Rock Mech. Min. Sci. 61, 96–110.
He, L., An, X.M., Zhao, Z.Y., 2015. Fully grouted rock bolts: an analytical investigation. Rock Mech. Rock Eng. 48, 1181–1196.
Horino, F.G., Ellickson, M.L., 1970. A method of estimating strength of rock containing planes of weakness. U.S. Bur. Mines Rep. Invest 7449.
Huang, S.L., Xu, J.S., Ding, X.L., et al., 2010. Study of layered rock mass composite model based on characteristics of structural plane and its application. Chinese J. Rock Mech. Eng. 29 (4), 743–756 (in Chinese).
Hyett, A.J., Bawden, W.F., Reichert, R.D., 1992. The effect of rock confinement on the bond strength of fully grouted cable bolts. Int. J. Rock Mech. Min. Sci. Geomech. Abstr. 29 (5), 503–524.
Indraratna, B., Kaiser, P.K., 1990. Analytical model for design of grouted rock bolts. Int. J. Numer. Anal. Meth. Geomech. 14, 227–251.
Karanam, U.M.R., Dasyapu, S.K., 2005. Experimental and numerical investigations of stresses in a fully grouted rock bolts. Geotech. Geol. Eng. 23, 297–308.
Kilic, A., Yasar, E., Atis, C.D., 2003. Effect of bar shape on the pull-out capacity of fully -grouted rockbolts. Tunn. Undergr. Space Technol. 18, 1–6.
Kilic, A., Yasar, E., Celik, A.G., 2002. Effect of grout properties on the pull-out load capacity of fully grouted rock bolt. Tunn. Undergr. Space Technol. 17, 355–362.
Kim, S.H., Pelizza, S., Kim, J.S., 2006. A study of strength parameters in the reinforced ground by rock bolts. Tunn. Undergr. Space Technol. 21, 378–379.
Li, C.C., Stjern, G., Myrvang, A., 2014. A review on the performance of conventional and energy-absorbing rockbolts. J. Rock Mech. Geotech. Eng. 6 315–227.
Li, D.Q., Masoumi, H., Saydam, S., et al., 2017. A constitutive model for load-displacement performance of modified cable bolts. Tunn. Undergr. Space Technol. 68, 95–105.
Li, S.C., Wang, G., Wang, S.G., et al., 2006.. Application of fracture-damage model to anchorage of discontinuous jointed rockmass of excavation and supporting. Chinese J. Rock Mech. Eng. 25 (8), 1582–1590 (in Chinese).
Li, Y., Zhou, H., Zhang, L., et al., 2016. Experimental and numerical investigations on mechanical property and reinforcement effect of bolted jointed rock mass. Constr. Build. Mater. 126, 843–856.
Liang, Z.Z., Tang, C.A., Li, H.X., Xu, T., Yang, T.H., 2005. A numerical study on failure process of transversely isotropic rock subjected to uniaxial compression. Rock Soil Mech. 26 (1), 57–62 (in Chinese).
Liu, Y.S., Fu, H.L., Wu, Y.M., et al., 2013. Experiment study of elastic parameters and compressive strength for transversely isotropic rocks. J. Central South Univ. (Sci. Technol.) 44 (8), 3398–3404 (in Chinese).
Liu, Q.S., Lei, G.F., Peng, X.X., et al., 2016. Advance and review on the anchoring mechanism in deep fractured rock mass. Chinese J. Rock Mech. Eng. 35 (2), 312–332 (in Chinese).
Liu, Q.S., Lei, G.F., Peng, X.X., et al., 2017. Experimental study and mechanism analysis of influence of bolt anchoring on shear properties of jointed rock mass. Rock Soil Mech. 36 (S1), 27–35 (in Chinese).
Maghous, S., Bernaud, D., Couto, E., 2012. Three-dimensional numerical simulation of rock deformation in bolt-supported tunnels: a homogenization approach. Tunn. Undergr. Space Technol. 31, 68–79.
Marence, M., Swoboda, G., 1995. Numerical model for rock bolts with consideration of joint movement. Rock Mech. Rock Eng. 28 (3), 145–165.
Mclamore, R., Gray, K.E., 1967. The mechanical behavior of anisotropic sedimentary rocks. Trans. Amer. Soc. Mech. Eng. Series B 62–76.
Meng, Q., Zhao, H.B., Ru, Z.L., 2014. Equivalent strength parameters and reliability analysis of circular tunnel with rock bolt supporting. Rock Soil Mech. 35 (S1), 437–442 (in Chinese).
Osgouir, R., 2006. Ground reaction curve of reinforced tunnel using a new elasto-plastic model. Ph.D Thesis. The Technical University of Turin, Turin.
Pellet, F., Egger, P., 1996. Analytical model for the mechanical behavior of bolted rock joints subjected to shearing. Rock Mech. Rock Eng. 29 (2), 73–97.
Ramamurthy, T., 1993. Strength and modulus responses of anisotropic rocks. In: Hudson, J.A. (Ed.), Comprehensive Rock Engineering, vol. 1. Oxford, Pergamon, pp. 313–329.
Shen, B., Barton, N., 1997. The disturbed zone around tunnels in jointed rock masses. Int. J. Rock Mech. Min. Sci. Geomech. Abstr. 34 (1), 117–125.
Spang, K., Egger, P., 1990. Action of fully-grouted bolts in jointed rock and factors of influence. Rock Mech. Rock Eng. 23, 201–229.
Srivastava, L.P., Singh, M., 2015. Effect of fully grouted passive bolts on joint shear strength parameters in a blocky mass. Rock Mech. Rock Eng. 48, 1197–1206.
Tien, Y.M., Kuo, M.C., 2001. A failure criterion for transversely isotropic rocks. Int. J. Rock Mech. Min. Sci. 38 (3), 399–412.
Tien, Y.M., Tsao, P.F., 2000. Preparation and mechanical properties of artificial

transversely isotropic rock. Int. J. Rock Mech. Min. Sci. 37, 1001–1012.
Tien, Y.M., Kuo, M.C., Juang, C.H., 2006. An experimental investigation of the failure mechanism of simulated transversely isotropic rocks. Int. J. Rock Mech. Min. Sci. 43, 1163–1181.
Wong, T.F., Wong, R.H.C., Jiao, M.R., et al., 2004. Micromechanics and rock failure process analysis. Key Eng. Mater. 261–263 (5), 39–44.
Wu, W.P., Feng, X.T., Zhang, C.Q., et al., 2012. Reinforcing mechanism and simulating method for reinforcing effects of systemically grouted bolts indeep-buried hard rock tunnels. Chinese J. Rock Mech. Eng. 31 (1), 2711–2712 (in Chinese).
Xi, D.Y., Chen, L., 1994. On anisotropic of rock in geophysics. Comput. Tech. Geophys. Geochem. Expl. 16 (1), 16–21 (in Chinese).
Yang, D.S., 2004. Numerical simulation analysis of equivalent bolt rock mass and its applications. Master Thesis. Institute of rock and soil mechanics, The Chinese Academy of Science, Wuhan, PR China (in Chinese).
Yang, S.L., Zhu, H.C., Liu, Z.D., 2001. A new constitutive model of the layered rock mass reinforced with bolts. Chinese J. Geotech. Eng. 23 (4), 427–430 (in Chinese).
Yang, T.Y., 1994. Analytical model for evaluating reinforcement efficiency of bolts in layered rock masses. Chinese J. Rock Mech. Eng. 13 (4), 309–317 (in Chinese).
Zhang, Y.J., Liu, Y.P., 2002. Constitutive relationship and failure criterion for bolted orthotropic rockmass. Acta Mech. Sin. 34 (5), 812–819.
Zhang, X.M., 2007. Anisotropic Characteristic of Rock Material and Its Effect on Stability of Tunnel Surrounding Rock. Ph.D Thesis. Central South University, Changsha, China (in Chinese).
Zhao, P.L., Yao, Z., 1990. The composite material constitutive model of bedded rocks. J. Lanzhou Univ. (Nat. Sci.) 26 (2), 114–118 (in Chinese).
Zhu, F.S., Zheng, Y.T., 1996. Support action analysis of tensioned and grouted bolts. Chinese J. Rock Mech. Eng. 15, 333–337 (in Chinese).
Zhu, J.M., Wang, L., Gu, J.C., et al., 1988. Modelling study on mechanical behavior of complex material consisted of rock and rockbolts. J. Chongqing Inst. Archit. Eng. 32 (2), 11–18 (in Chinese).
Zhu, W.S., Ren, W.Z., 2001. Research on reinforcing effect for jointed rock masses of shiplock slope by physical modeling. Chinese J. Rock Mech. Eng. 20 (5), 720–725 (in Chinese).